Phase diagrams of the spin-2 Ising model in the presence of a quenched diluted crystal field distribution

Ali Yigit[a)†] and Erhan Albayrak[b)]

[a)] *Çankiri Karatekin University, Department of Physics, Çankiri* 18100, *Turkey*
[b)] *Erciyes University, Department of Physics, Kayseri* 38039, *Turkey*

(Received 25 April 2012)

We have investigated the random crystal field effects on the phase diagrams of the spin-2 Blume–Capel model for a honeycomb lattice using the effective-field theory with correlations. To do so, the thermal variations of magnetization are studied via calculating the phase diagrams of the model. We have found that the model displays both second-order and first-order phase transitions in addition to the tricritical and isolated points. Reentrant behavior is also observed for some appropriate values of certain system parameters. Besides the usual ground-state phases of the spin-2 model including ± 2, ± 1, and 0, we have also observed the phases $\pm 3/2$ and $\pm 1/2$, which are unusual for the spin-2 case.

Keywords: spin-2 model, random crystal field, effective-field theory, isolated critical points and triciritical points

PACS: 05.40.−a, 05.50.+q, 64.60.De **DOI:** 10.1088/1674-1056/21/11/110503

1. Introduction

It is well known that analysis of spin models becomes very difficult as the spin values increase. Therefore, it is less attractive for high-spin models than lower-spin models. We have also observed the same problem in the relevant literatures regarding the random crystal field (RCF) in the spin-2 case.

The crystal field (CF) considerably affects the critical behavior of the system. If it is strong enough, the energy difference between the split levels is large. In this case, it is more favorable to put as many electrons as possible into lower energy levels before one starts to fill higher energy levels. Filling all the orbitals in lower levels means that electrons are arranged in pairs, with opposite spins within each orbital. Electron pairs with opposite spins make no contribution to the total spin, resulting in a lower-spin state. Thus, its competition with the bilinear interaction parameter leads to first-order phase transitions. Usually, a CF is considered to be constant throughout the lattice. Nowadays, RCFs with a probability distribution instead of a constant one has become popular for investigations. The randomness and distribution type of the CF may greatly affect the critical behavior of the system. Therefore, we are dedicated to studying the spin-2 Blume–Capel (BC) model with an RCF.

Because of the difficulties in studying high-spin models, the spin-2 model with a constant CF has received less attention than it deserves. Therefore, a small number of techniques have been employed to deal with such models. A new effective-field theory (EFT) was developed for high-spin models with a CF,[1] and the general expression for evaluating the transition line T_c and tricritical point was formulated for the spin-2 BC model. The general BC models with integer and semi-integer spins were studied using the mean field theory (MFT).[2] The physical properties of the spin-2 model with a biaxial CF on the simple body-centered and face-centered cubic lattices were studied using the EFT with self-spin correlations and the differential operator technique.[3] The ferromagnetic spin-2 random-field Ising model in the presence of a CF on honeycomb, square, and simple cubic lattices was examined within the framework of the EFT with correlations.[4] The transverse spin-2 Ising model with a CF was investigated within the EFT with correlations.[5] The phase diagrams and magnetization curves[6] as well as the ground-state phase diagrams of the transverse spin-2 Ising model with a longitudinal CF were obtained using the MFT based on the Bogoliubov inequality for the Gibbs free energy.[7] The kinetic spin-2 BC model under a time-dependent oscillating magnetic field was studied using the EFT with correlations[8] and the MFT.[9]

However, we note that there is only one piece of

†Corresponding author. E-mail: ayigit80@karatekin.edu.tr
© 2012 Chinese Physical Society and IOP Publishing Ltd

work[10] which includes the effects of an RCF on the spin-2 BC model and uses the double-peaked delta distribution

$$P(\Delta_i) = \frac{1}{2}\{\delta(\Delta_i - \Delta(1+\alpha)) + \delta(\Delta_i - \Delta(1-\alpha))\},$$

where Δ_i is an RCF and α ($\alpha \geq 0$) is a parameter that provides the fluctuation of the crystal field. The phase diagrams and the thermal variations of magnetization of the model were investigated using the MFT. As a result, the model yields triciritical points and double critical end points. However, they did not discover the unusual phase $\pm 1/2$, which are the main findings in our work.

The remaining part of this work is organized as follows. Section 2 is devoted to the explanation and formulation of the model. Section 3 presents our findings, followed by a brief summary given in Section 4.

2. Formulation

The Hamiltonian of the spin-2 BC model is given by

$$\mathcal{H} = -J\sum_{\langle i,j\rangle} S_i S_j + \sum_i D_i S_i^2, \tag{1}$$

where S_i is the spin at site i, which takes the discrete values ± 2, ± 1, and 0. The first sum runs over all pairs of nearest-neighbor (NN) sites. The J is the bilinear interaction parameter between the NN spins, and D_i is the site-dependent CF. The probability distribution used in this paper is called a quenched diluted crystal field distribution, which has been used in dealing with spin-1 Ising models examined using the EFT with correlations.[11,12] The quenched diluted crystal field distribution is given by

$$P(D_i) = p\delta(D_i - D) + (1-p)\delta(D_i), \tag{2}$$

where $D_i = D/J$. With this random CF distribution, the CF is either turned on or turned off with given probabilities p and $1-p$, respectively, on the lattice sites.

The magnetization of the spin-2 Ising model is obtained here by means of the widely-used EFT with correlations, first introduced by Honmura and Kaneyoshi,[13] and Kaneyoshi *et al.*[14] In the EFT, the thermal and configurational average of the lattice magnetization is given by

$$\begin{aligned} M &= \langle\langle S_i\rangle\rangle_r \\ &= \left\langle\left\langle \prod_{i=1}^{z}[1 + A(\alpha)S_i + B(\alpha)(S_i)^2 \right.\right. \\ &\quad \left.\left. + C(\alpha)(S_i)^3 + D(\alpha)(S_i)^4]\right\rangle\right\rangle_r \\ &\quad \times F(x)|_{x=0}, \end{aligned} \tag{3}$$

where $\alpha = J\nabla$, $\nabla = \partial/\partial x$ is the differential operator, and z denotes the nearest-neighbor site of the central site i and $z = 3$ on the honeycomb lattice. The coefficients $A(\alpha)$, $B(\alpha)$, $C(\alpha)$, and $D(\alpha)$ can be calculated using the van der Waerden identities.[1] They are expressed as

$$\begin{aligned} A(\alpha) &= \frac{1}{6}[8\sinh(\alpha) - \sinh(2\alpha)], \\ B(\alpha) &= \frac{1}{12}[16\cosh(\alpha) - \cosh(2\alpha) - 15], \\ C(\alpha) &= \frac{1}{6}[\sinh(2\alpha) - 2\sinh(\alpha)], \\ D(\alpha) &= \frac{1}{12}[\cosh(2\alpha) - 4\cosh(\alpha) + 3]. \end{aligned} \tag{4}$$

The function $F(x)$ in Eq. (3) is defined as

$$F(x) = \int P(D_i) f(x, D_i) \mathrm{d}D_i, \tag{5}$$

where $f(x, D_i)$ for the spin-2 model is given by

$$\begin{aligned} &f(x, D_i) \\ &= \frac{4\sinh(2\beta x) + 2\sinh(\beta x)\exp(3\beta D_i)}{2\cosh(2\beta x) + 2\cosh(\beta x)\exp(3\beta D_i) + \exp(4\beta D_i)}, \end{aligned} \tag{6}$$

where $\beta = 1/(kT)$ with k being the Boltzman constant, and T being the absolute temperature.

When the right-hand side of Eq. (3) is expanded, the multi-spin correlation functions appear, making the problem much more difficult. In order to ignore these correlations, one can use the decoupling approximation

$$\langle\langle S_i S_{i'} \cdots S_{i^n}\rangle\rangle_r \cong \langle\langle S_i\rangle\rangle_r \langle\langle S_{i'}\rangle\rangle_r \cdots \langle\langle S_{i^n}\rangle\rangle_r \tag{7}$$

for $i \neq i' \neq \cdots \neq i^n$.[15] This approximation corresponds to Zernike approximation in a crystalline Ising ferromagnet.[16] Within the decoupling approximation, Eq. (3) for z=3 is given by

$$\begin{aligned} M &= \langle\langle S_i\rangle\rangle_r \\ &= [1 + A(\alpha)\langle\langle S_i\rangle\rangle_r + B(\alpha)\langle\langle S_i^2\rangle\rangle_r \\ &\quad + C(\alpha)\langle\langle S_i^3\rangle\rangle_r + D(\alpha)\langle\langle S_i^4\rangle\rangle_r]^3 \\ &\quad \times F(x)|_{x=0}. \end{aligned} \tag{8}$$

Expanding the right-hand side of Eq. (8) and according to an approximation that $\langle\langle (S)^n\rangle\rangle_r = M^n$ used in Refs. [8] and [17], one can obtain

$$M = a_0 + a_1 M + a_2 M^2 + a_3 M^3$$

$$+ a_4M^4 + a_5M^5 + a_6M^6 + a_7M^7 + a_8M^8 + a_9M^9 + a_{10}M^{10} + a_{11}M^{11} + a_{12}M^{12}, \quad (9)$$

where the coefficients $a_0, a_1, \ldots, a_9$ are easily obtained using the mathematical relation $\exp(\gamma\nabla)F(x) = F(x+\gamma)$. It is also feasible to introduce the quadrupolar order parameter, but for the purpose of our study the magnetization is good enough.

Based on the formula obtained above for the EFT with correlations, we are now ready to carry out calculations for the case of the RCF given by Eq. (2). The calculations are carried out within an iteration scheme because of the nature of the equations for magnetization when $z = 3$. In the next section, the topological phase diagrams and our findings are presented, which are obtained by studying the thermal variations of magnetization for given constant values of our system parameters.

3. Thermal variations of magnetization, and phase diagrams

In order to obtain evidence for the existence of the ground-state phases $\pm 3/2$ and $\pm 1/2$, which are unusual for a spin-2 system, we have studied the thermal variations of magnetization. As shown in Fig. 1, the magnetization starts from the ground-state values, i.e., the values of magnetization at zero temperature: $M = 2.0$ for $D/J = 1.0$ and $p = 0.5$, $M \simeq 1.5$ for $D/J = 2.0$ and $p = 0.6$, $M = 1.0$ for $D/J = 8.0$ and $p = 0.5$, and $M \simeq 0.5$ for $D/J = 10.0$ and $p = 0.8$. All the magnetization curves only exhibit second-order phase transitions, and the temperature T_c is higher for magnetization with higher ground-state values. We also note that these curves separate the ordered phases from the disordered phases and the paramagnetic phase.

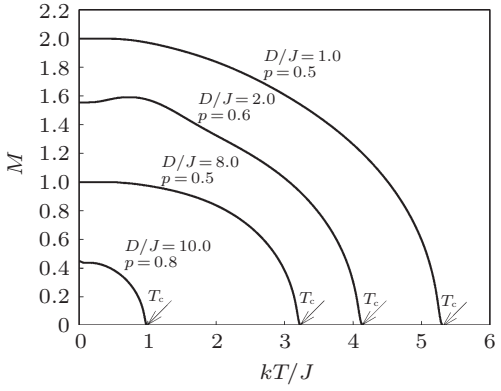


Fig. 1. Temperature variations of magnetization for $z = 3$.

Figure 2 illustrates the existence of the reentrant behavior. It can be seen that M is about 1.5 at zero temperature. As the temperature rises, the M decreases and then jumps to zero at the first-order phase transition temperature T_t. Later, the magnetization remains zero until the first second-order phase transition temperature T_{c1}, where a peak occurs. Then, it goes to zero again at the second second-order phase transition temperature T_{c2}. The existence of two second-order phase transition temperatures leads to the reentrant behavior in the phase diagram.

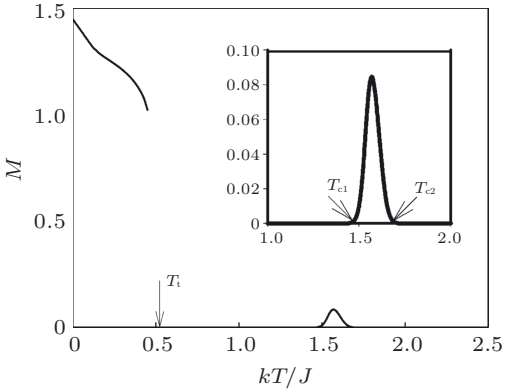


Fig. 2. Thermal variation of magnetization for $z = 3$, $D/J = 2.057$, and $p = 0.9$.

Figure 3 also displays the thermal variations of magnetization, showing the existence of the first-order phase transitions and also the type of the phases involved in these transitions. Figure 3(a) shows that the magnetization starts from ~ 1.0 at zero temperature for $D/J = 1.33$ and $p = 0.9$. The magnetization increases with increasing temperature first, and jumps to ~ 2.0 at the first-order phase transition temperature T_t. Then it decreases with increasing temperature, and goes to zero at the second-order phase transition temperature. All these phenomena can be expressed as $\{(F_1, F_2)_{T_t}, (F_2, P)_{T_c}\}$, where F and P refer to the ferromagnetic phase and the paramagnetic phase, respectively. Subscripts 1 and 2 represent the ground-state spin values and the subscripts T_c or T_t denote the types of phase transition. Figure 3(b) shows that the model displays two T_t and a T_c. Now the story is simply given by $\{(F_1, F_0)_{T_{t1}}, (F_0, F_{1/2})_{T_{t2}}, (F_{1/2}, P)_{T_c}\}$. Similarly, Figs. 3(c), 3(d), and 3(e) tell us the stories $\{(F_{3/2}, P)_{T_t}\}$,$\{(F_{1/2}, F_{3/2})_{T_{t1}}, (F_{3/2}, F_1)_{T_{t2}}, (F_1, P)_{T_c}\}$, and $\{(F_1, F_{3/2})_{T_t}, (F_{3/2}, P)_{T_c}\}$, respectively. It is also obvious that we not only obtain the usual ground-state phases but also the unusual ones.

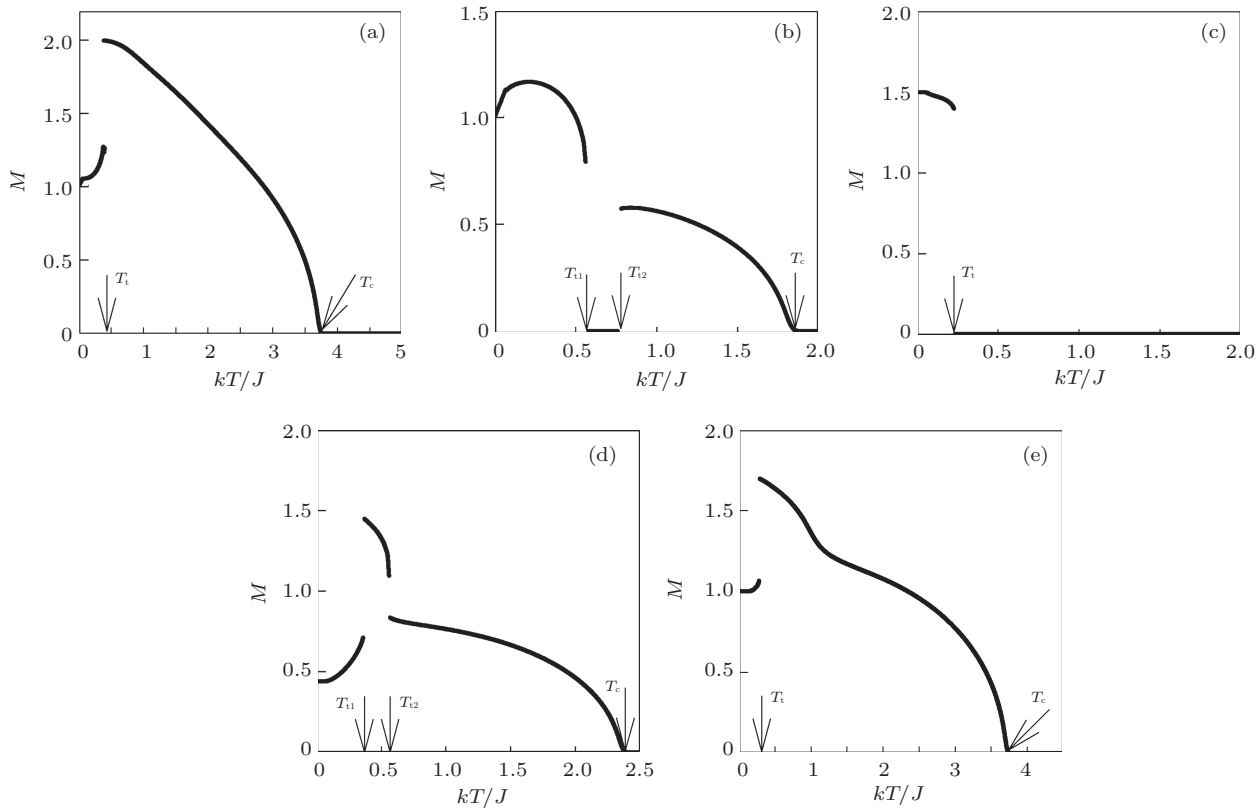


Fig. 3. Temperature variations of magnetization for $z = 3$ with (a) $D/J = 1.33$, $p = 0.9$, (b) $D/J = 1.97$, $p = 0.9$, (c) $D/J = 2.95$, $p = 0.9$, (d) $D/J = 2.4, p = 0.8$, and (e) $D/J = 3.9$, $p = 0.5$.

After studying the thermal variations of magnetization, we are now ready to obtain the phase diagrams, which are simply a collection of the phase-transition temperatures for given system parameters. They are obtained on the D/J–kT/J plane for given values of p when $z = 3$. They are calculated in the range between p=0 and $p = 1.0$ with a step of $\Delta p = 0.1$. In the phase diagrams (see Figs. 4 and 5), the solid and dotted lines represent the second-order and first-order phase transition lines, while the filled triangle and empty circle represent the tricritical and isolated points, respectively. It should be mentioned that $p = 0.0$ means that the CF is turned off throughout the lattice, in which case the model is left with the bilinear interaction parameter J and temperature. Since all the parameters are divided by J to reduce the system parameters by one and usually this is equal to setting $J = 1$. Therefore, when $p = 0$, only one T_c line is expected to be seen at constant temperature, which is actually the case shown in Fig. 4(a). This line separates the F_2 phase from the P phase as expected. The other extreme case corresponds to $p = 1.0$ at which all of the lattice sites are under the effect of the same CF. In other words, the model reduces to the well-known BC model. Figure 4(b) shows for $p = 1.0$ that the T_c line combines with the T_t line at the tricritical point. In addition, the second T_t line slants to the right and terminates at the isolated point. This figure is similar to Fig. 2 in Ref. [2] and Fig. 3 in Ref. [6], but their T_t lines start from the same D/J values at zero temperature, which is distinct from our resuls. For the remaining p values, the CF randomly acts on the lattice sites. In other words, it is randomly turned on or off for each site. Therefore, it is now called the RCF. We know that there is strong competition between J, which is simply set to 1, and the CF values. When the CF is much larger than $J = 1$, it is possible for the spins to pair up to lower the magnetization, but J tends to align the spins to increase the magnetization (see Eq. (1)). Thus, the temperatures of the critical lines decrease. However, when the CF is negative, there is no competition with J. They support each other, leading to the increase in the critical temperature. The above points are illustrated in Figs. 4(c)–4(f) when $p = 0.1, 0.2, 0.3$, and 0.4, respectively. It is clear that the temperatures of the T_c lines are reduced for higher positive CF values, and then increase when the negative CF deceases to a certain value. In addition, the T_c lines are seen at lower temperatures for high positive values of p and D/J, but the lines are seen at higher temperatures for high values of p when D/J is negative. Note that the T_c lines separate F_2

phase from the P phase for all p values except $p = 0.4$. In the latter case, the T_c lines separate the F_2 phase from the P phase at lower D/J, and separate the $F_{3/2}$ phase from the P phase for higher D/J values.

In Figs. 5(a)–5(e), the T_c lines appear at higher temperatures for $p = 0.5, 0.6, 0.7$, and 0.8, whose behaviors are similar to those in Figs. 4(a)–4(f), where all the T_t lines terminate at isolated points. Figure 5(a) shows the ground states $F_2, F_{3/2}$, and F_1, and the T_t line separating the phases $F_{3/2}$ and F_1 terminates at an isolated point. In Figs. 5(b) and 5(c), we see an extra T_t line separating phases F_1 and $F_{3/2}$, compared with Fig. 5(a). Figure 5(d) exhibits three T_t lines, which corresponds to $\{(F_2, F_1)_{T_t}\}$, $\{(F_1, F_{3/2})_{T_t}\}$, and $\{(F_{3/2}, F_{1/2})_{T_t}\}$ in increasing order of temperature.

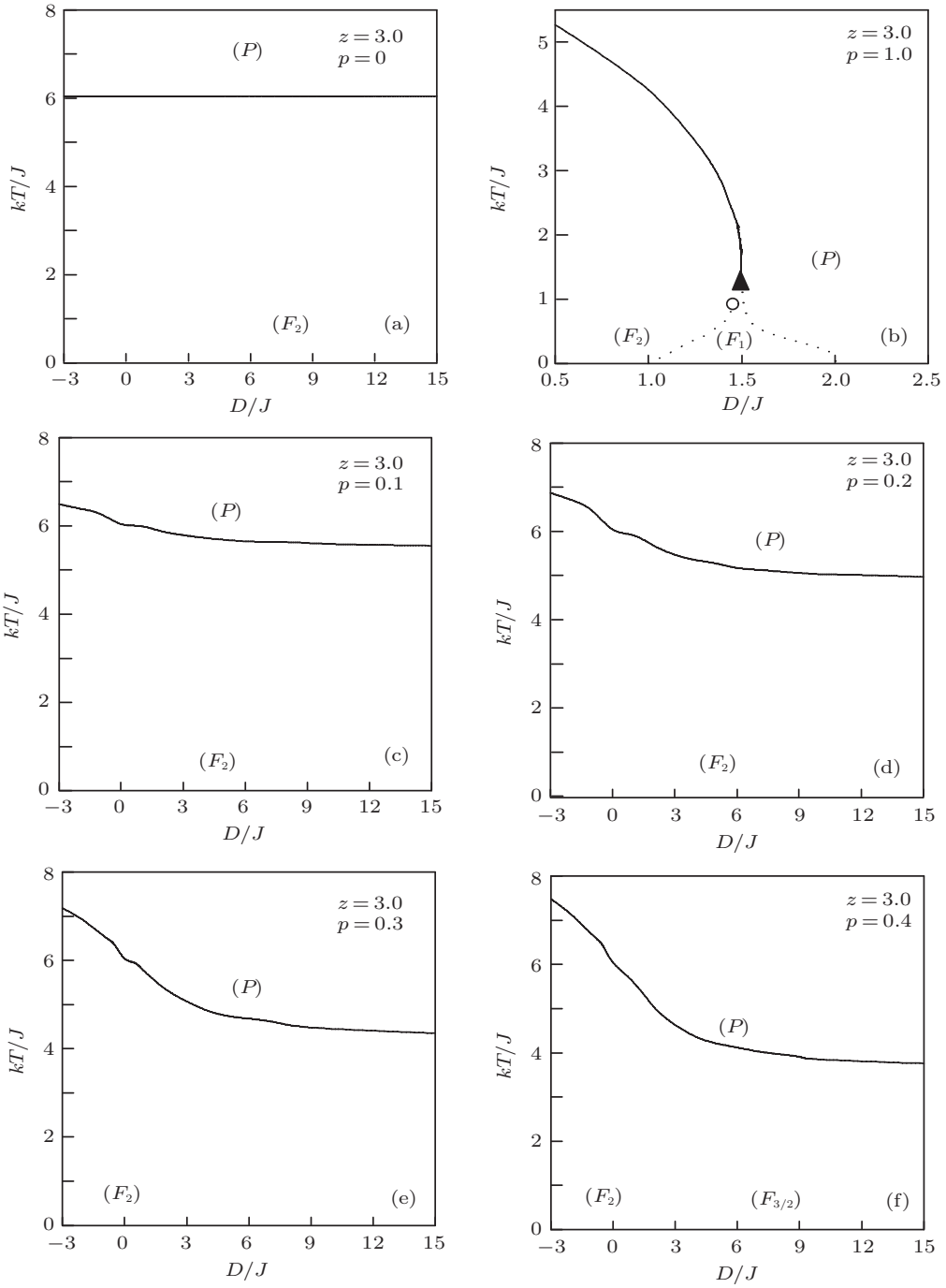


Fig. 4. Phase diagrams of the spin-2 RCF model on the $(D/J, kT/J)$ planes for $z = 3$. (a) $p = 0.0$, (b) $p = 1.0$, (c) $p = 0.1$, (d) $p = 0.2$, (e) $p = 0.3$, and (f) $p = 0.4$.

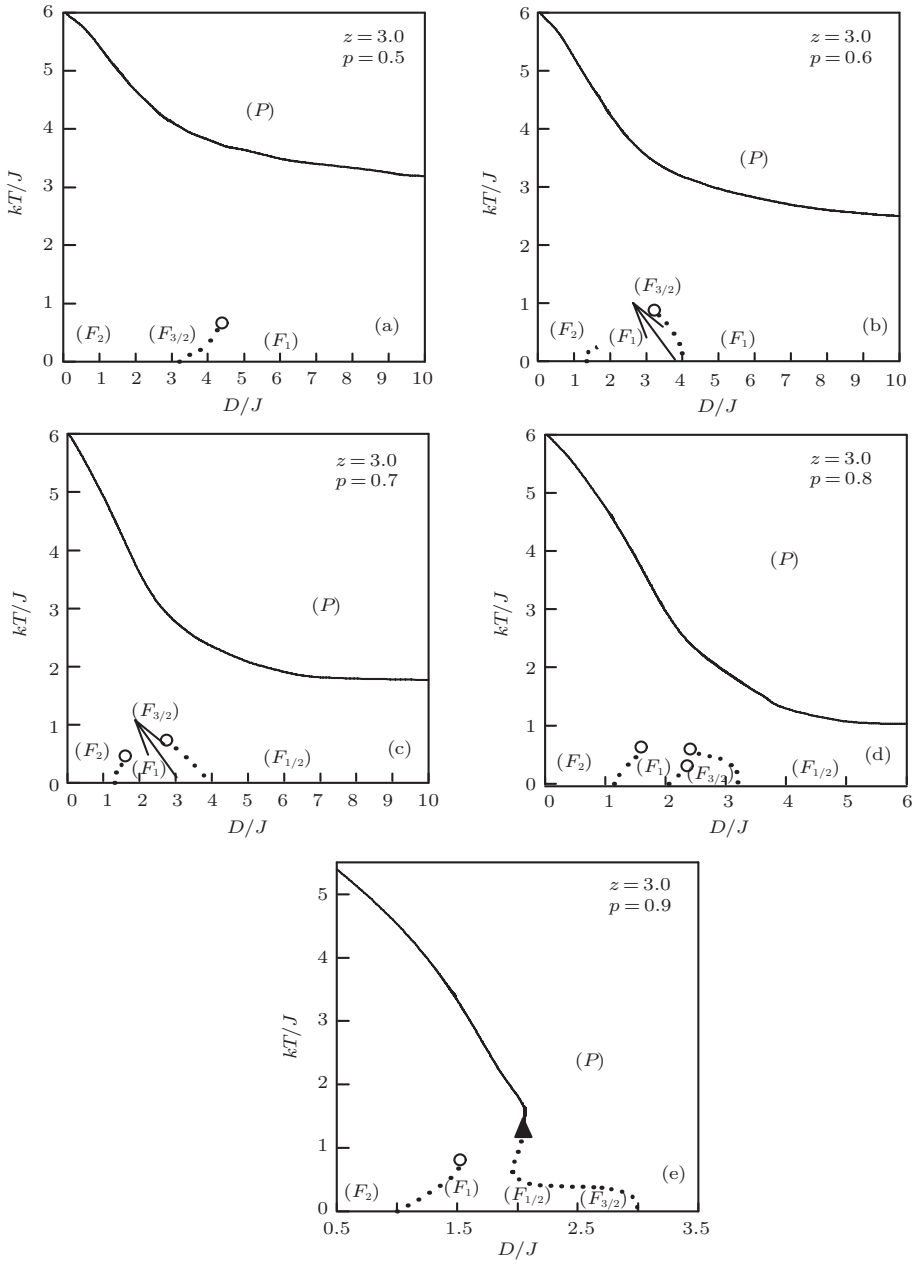


Fig. 5. Phase diagrams of the spin-2 RCF model on the $(D/J, \mathrm{k}T/J)$ planes for $z = 3$. (a) $p = 0.5$, (b) $p = 0.6$, (c) $p = 0.7$, (d) $p = 0.8$, and (e) $p = 0.9$.

The last phase diagram of this work is obtained for $p = 0.9$ (see Fig. 5(e)). It is similar to Fig. 4(b) except that the T_{t} line terminating at the tricritical point shows somewhat wiggly behavior in Fig. 4(b). In addition, we see all four ground-state configurations: F_2, F_1, $\mathrm{F}_{3/2}$, and $\mathrm{F}_{1/2}$. In Fig. 4(b), only the phases F_2 and F_1 are seen.

4. Conclusion

In conclusion, we have investigated the RCF effects on the phase diagrams of the spin-2 BC model for the honeycomb lattice using the EFT with correlations. The thermal changes of magnetization were studied, and thus the phase diagrams of the model were obtained. It was found that the model exhibits both second-order and first-order phase transitions in addition to the tricritical and isolated points. The reentrant behavior was also observed. We briefly state what we have found in the presence of an RCF below.

i) As the probability p decreases, the tricritical and isolated points disappear in the phase diagrams.

ii) With decreasing values of p ($p \leq 0.4$), the lines of first-order phase transition vanish, only the lines of

second-order phase transition in the phase diagrams are left. Thus, the complexity of the phase diagrams diminishes with decreasing p.

iii) The reentrant behavior occurs for a small range of CF values at about $p = 0.9$.

iv) In addition to the usual ground-state phases of a spin-2 system, specifically ± 2, ± 1, and 0, the phases $\pm 3/2$ and $\pm 1/2$ were also observed, which are unusual for the spin-2 case.

Finally, we should mention that there is only one work[10] in which a doubly-peaked distribution of the crystal field is used instead of our quenched diluted distribution. Our latest result shows that the spin-2 model has a ground state with spin 1/2, yet this is not observed in Ref. [10]. The ground state with spin 3/2 is found in both pieces of work. We hope that this work may inspire other researchers to study this model using different techniques.

References

[1] Kaneyoshi T, Tucker J W and Jaščur M 1992 *Physica* A **186** 495

[2] Plascak J A, Moreira J G and sáBarreto F C 1993 *Phys. Lett.* A **173** 360

[3] Jiang W, Guo A B, Li X, Wang X K and Bai B D 2006 *Commun. Theor. Phys.* **46** 1105

[4] Liang Y Q, Wei G Z, Zhang Q and Song G L 2004 *Chin. Phys. Lett.* **21** 378

[5] Jiang W, Wei G Z and Xin Z H 2000 *J. Magn. Magn. Mater.* **220** 96

[6] Zhao J, Xu X G and Wei G Z 2009 *Commun. Theor. Phys.* **52** 163

[7] Zhao J, Wei G Z and Xu X G 2006 *Commun. Theor. Phys.* **45** 749

[8] Ertas M, Deviren B and Keskin M 2012 *J. Magn. Magn. Mater.* **324** 704

[9] Keskin M, Canko O and Ertas M 2007 *J. Exp. Theor. Phys.* **105** 1190

[10] Bahmad L, Benyoussef A and El Kenz A 2007 *Phys. Rev.* B **76** 094412

[11] Yüksel Y, Akinci U and Polat H 2012 *Physica* A **391** 2819

[12] Gulpinar G, Vatansever E and Agartioglu M 2012 *Physica* A (in press)

[13] Honmura R and Kaneyoshi T 1979 *J. Phys.* C **12** 3979

[14] Kaneyoshi T, Fittipaldi I P, Honmura R and Manabe T 1981 *Phys. Rev.* B **24** 481

[15] Tamura I and Kaneyoshi T 1981 *Prog. Theor. Phys.* **66** 1892

[16] Zernike F 1940 *Physica* **1** 565

[17] Ertas M, Keskin M and Deviren B 2012 *J. Magn. Magn. Mater.* **324** 1503